

# Cotton-derived carbon fibers with high specific capacitance by $\text{ZnCl}_2$ activation for supercapacitor application

Shuguang Wang<sup>1,a</sup>, JieYu<sup>1,b</sup>

<sup>1</sup> Shenzhen Engineering Laboratory for Supercapacitor Materials, Shenzhen Key Laboratory for Advanced Materials, Department Material Science and Engineering, Shenzhen Graduate School, Harbin Institute of Technology, University Town, Shenzhen 518055 China.

<sup>a</sup> wangshug2011@163.com; <sup>b</sup> jyu@hitsz.edu.cn

**Keywords:** Porous carbon fibers; cotton; supercapacitors;  $\text{ZnCl}_2$ ; high specific capacitance

**Abstract.** Cotton, an inexpensive natural product, was used as a precursor for fabrication of high specific capacitance porous carbon fibers for supercapacitors. Porous carbon fibers with the hollow structure, high surface area of  $1620 \text{ m}^2 \text{ g}^{-1}$  and high content of C=O functional group are prepared by one-step carbonization and activation using  $\text{ZnCl}_2$  as activation agent. The maximum specific capacitance of porous carbon fibers activated at a  $\text{ZnCl}_2$ /cotton mass ratio of 2:1 is measured to be  $426.7 \text{ F g}^{-1}$  at a current density  $0.6 \text{ A g}^{-1}$ . The tubular structure, high surface area, and high content of oxygen functional groups are responsible for the excellent electrochemical performance.

## Introduction

As a new class of energy storage devices, supercapacitors are attracting an increasing interest due to their advantages of high power capability, long cycle life, fast charge and discharge rate, and low cost [1-4]. Therefore, much effort has been devoted to developing active electrode materials for supercapacitors. Various carbon materials such as activated carbon [5, 6], carbon nanotubes [7], carbon fibers (CFs) [8, 9], and graphene [10] are generally used as electrode materials for supercapacitors. Conventional CFs are generally prepared from pitch or polyacrylonitrile, which have been used for supercapacitor applications after activation and shows better electrochemical performance than the granular activated carbon due to their fibrous morphology [11]. However, the preparation procedures of the activated CFs need both carbonization and activation, which is high cost and not environmentally friendly. Compared with the conventional CFs, the cotton-based CFs (CCFs) is hollow and may have better electrochemical performance when used as the active materials due to the increase surface area [8]. Anyway, the CCFs provide an alternative choice for flexible supercapacitor application due to the green nature, good mechanical properties and low cost [9]. However, the reported CCFs have low specific capacitance because of the low specific surface area. At present, the preparation of porous CCFs with high specific surface area and high specific capacitance have not been well investigated, and thus further work is necessary to exploit the capability of the CCFs by modifying their structure.

In this paper, we report a facile, cost-effective method to prepare porous CCFs with hollow structure from cotton by a one-step carbonization and activation process. We used  $\text{ZnCl}_2$  as activation agent to enhance specific surface area. The results demonstrate that porous CCFs present a promising electrode materials with high specific capacitance of  $426.7 \text{ F g}^{-1}$  in  $1 \text{ M H}_2\text{SO}_4$ .

## Experimental

The cotton was obtained from Hualu Company in Shandong province. Porous CCFs were obtained by one-step carbonization and activation method. First, the cotton was impregnated in  $\text{ZnCl}_2$  solution for 6 h with different  $\text{ZnCl}_2$ /cotton mass ratios, where the cotton mass used was 2 g. Then, the  $\text{ZnCl}_2$ -impregnated cotton was carbonized at  $850 \text{ }^\circ\text{C}$  for 2 h in  $60 \text{ mL min}^{-1}$  nitrogen flow by conventional heating. As a contrast, the cotton was carbonized following the above described procedure. The CCFs were denoted as CCFs0, CCFs1, CCFs2, and CCFs3, which the  $\text{ZnCl}_2$ /cotton

mass ratios are 0/1, 1/1, 2/1, and 3/1, respectively. The materials characterization and electrochemical measurement were referenced previously reported literature [8].

## Result and discussion

The SEM images of the CCFs0 and CCFs2 are shown in the Fig. 1. The diameter of the CCFs0 is 6-8  $\mu\text{m}$ , similar to that of commercial Nomex aramid CFs [8]. The fiber morphology of the CCF2 is well preserved after activation, and the average diameter of the CCFs2 is similar to CCFs0.

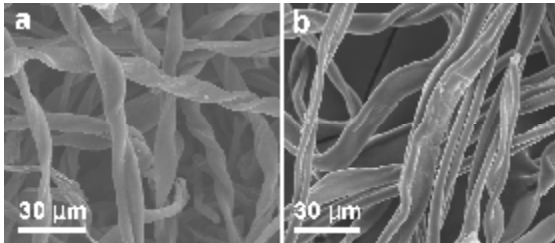


Fig. 1. SEM images of CCFs0 (a) and CCFs2 (b).

Nitrogen adsorption/desorption isotherms and the pore size distribution of the different samples are shown in Fig 2. The pore structure parameters of samples in different yield are presented in table 1. All the isotherms in Fig. 2a show the characteristic type I isotherm according to the IUPAC classification. While, the CCFs with  $\text{ZnCl}_2$ /cotton mass ratio at 2 and 3 show an apparent adsorption/desorption hysteresis loop at  $P/P_0$  value of 0.40-0.55, which are caused by the capillary condensation in mesopores [12]. It is seen that the specific surface area and the adsorption volumes of the CCFs increase with the  $\text{ZnCl}_2$ /cotton mass ratio from 1 to 3. The specific surface area of the CCFs with  $\text{ZnCl}_2$ /cotton mass ratio from 1 and 3 are 1303.6, 1600.4, and 1620.0  $\text{m}^2 \text{g}^{-1}$ , respectively. In contrast, the CCFs0 without adding  $\text{ZnCl}_2$  during carbonization show much lower adsorption capacity with a specific surface area of 89.6  $\text{m}^2 \text{g}^{-1}$ . It is noted that the CCFs activated by  $\text{ZnCl}_2$  possess higher mesopore percentage than the activated carbon prepared by the KOH [13], which is beneficial for supercapacitor applications [8, 14]. The pore size distribution of CCFs2 and CCF3 in Fig. 2b shows a bimodal distribution of above 2 nm micropore and along with a large proportion around 3.4 nm mesopores. The mesopore percentage of the CCFs0 is only 14%. The mesopore percentage of CCFs increases with the increase in the  $\text{ZnCl}_2$ /cotton mass ratio from 1 to 3, indicating that the porosity created by  $\text{ZnCl}_2$  activation is due to the space activated and left by  $\text{ZnCl}_2$  after washing [15]. The average pore size increases from 1.97 to 2.65 nm, and the yield decrease from 26.2 % to 23.1% with increase of the  $\text{ZnCl}_2$ /cotton mass ratio from 1 to 3 (Table 1). The increase of the average pore size and mesopore volume of activated CCFs can be related to the intense chemical attacking of carbon by more  $\text{ZnCl}_2$ , which leads to the decrease of the yield of activated CCFs. The high surface area along with a bimodal size distribution comprising of micropores and mesopores is interesting from the standpoint of supercapacitor application, as will be discussed later.

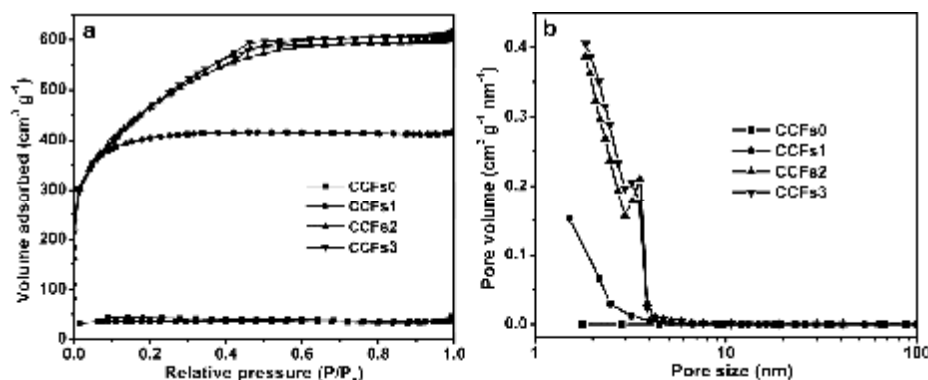


Fig. 2. Nitrogen adsorption/desorption isotherms (a) and pore size distribution (b) of the CCFs0, CCF1, CCF2 and ACCF3.

**Table 1.** Calculated total specific surface area ( $S_t$ ,  $m^2 g^{-1}$ ), micropore specific surface area ( $S_m$ ,  $m^2 g^{-1}$ ), total pore volume ( $V_t$ ,  $cm^3 g^{-1}$ ), micropore volume ( $V_m$ ,  $cm^3 g^{-1}$ ), average pore size ( $d_a$ , nm), mesopore percentage ( $V_{meso}/V_t$ , %), and yeild (%) of the the CCFs0, CCFs1, CCFs2, and CCF3.

samples	ZnCl <sub>2</sub> :Cotton	$S_t$	$S_m$	$V_t$	$V_m$	$d_a$	$V_{meso}/V_t$	Yeild
CCFs0	0:1	89.6	70.5	0.065	0.056	28.79	14	30.2
CCFs1	1:1	1303.6	943.0	0.643	0.464	1.97	28	26.2
CCFs2	2:1	1600.4	235.1	0.931	0.120	2.32	87	24.9
CCFs3	3:1	1620.0	120.9	0.992	0.063	2.65	94	23.1

XPS spectra were measured to identify the composition and oxygen doping states of the obtained samples. Fig. 3 shows the XPS survey spectra and the O1s XPS spectra of the all samples. The relative percentages of carbon, oxygen, nitrogen and oxygen-containing functional groups in samples are presented in Table 2. In comparison to the relative percentage of the carbon and oxygen, the nitrogen content of samples is smaller than 0.5%, and may be ignored. It is worthy to note that C=O and C-O functional groups are the main oxygen-containing functional groups in all samples, and that the relative percentages of C=O and C-O functional groups in CCFs1 and CCF2 are higher than that in CCFs3. According to the literature, the C=O and C-O functional groups will contribute to the electrochemical capacitance by introducing Faradaic reactions and improving the wettability [8, 16, 17].

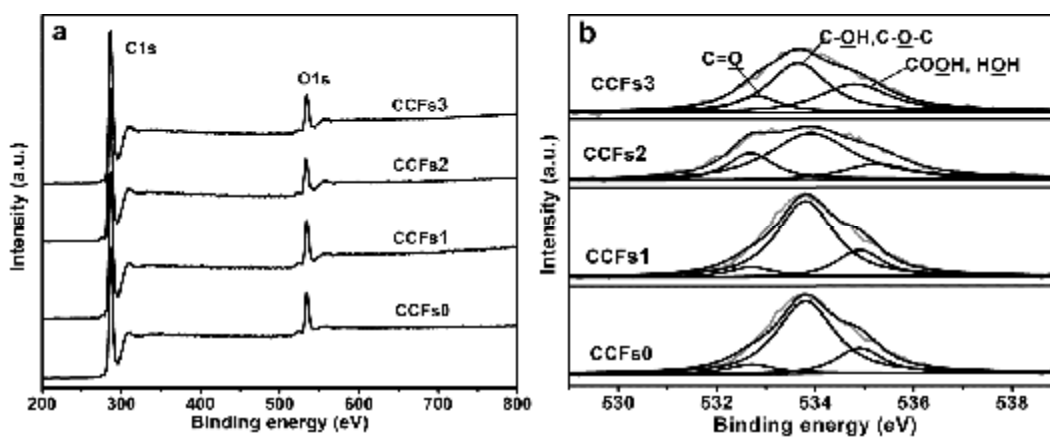


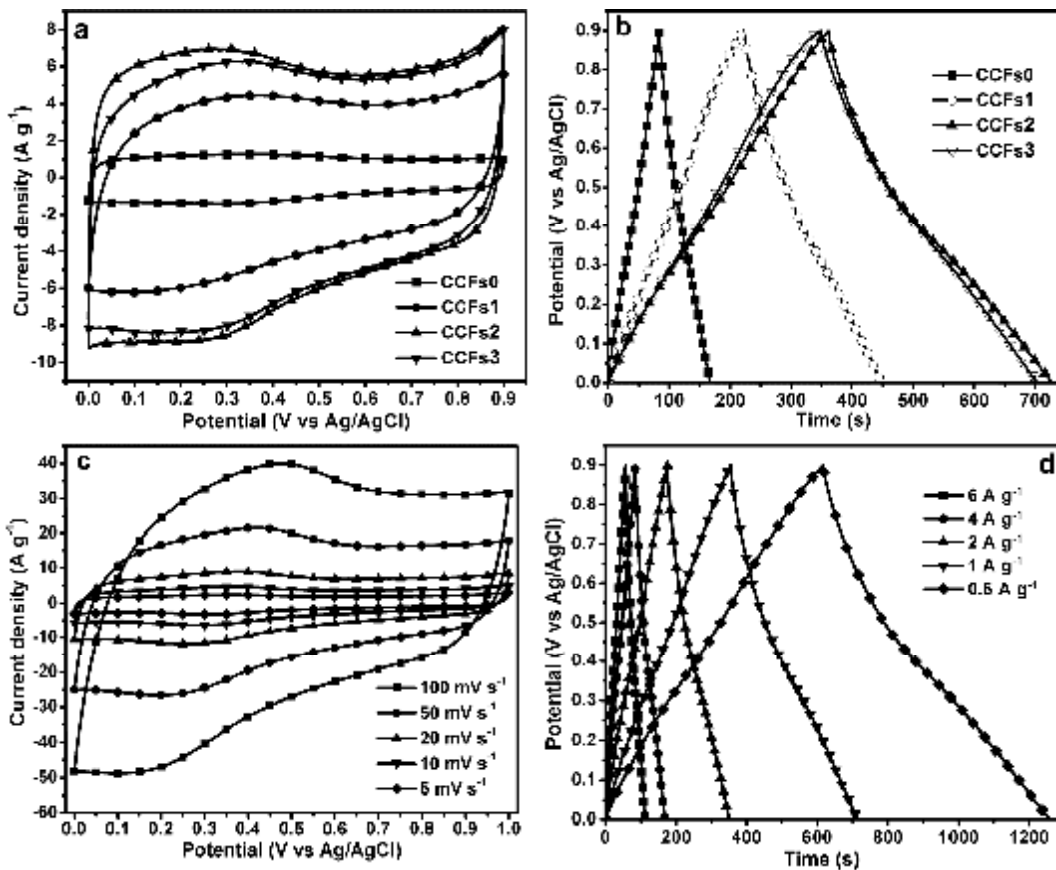
Fig. 3. XPS survey spectra (a) and O1s spectra (b) of the samples.

Table 2 Relative percentages of carbon, oxygen, nitrogen, and oxygen-containing functional groups of the samples obtained by XPS.

Samples	C	O	N	O1s		
				C=O	C-OH, C-O-C	COOH, HOH
CCFs0	89.17	10.54	0.29	4.3	44.8	50.9
CCFs1	89.84	9.90	0.26	8.5	71.4	20.1
CCFs2	89.20	10.38	0.42	20.7	63.5	15.8
CCFs3	92.53	7.2	0.27	13.7	51.7	31.6

Electrochemical performance of the CCFs was first evaluated in 1 M H<sub>2</sub>SO<sub>4</sub> solution using a three-electrode system. The Cyclic voltammetry (CV) curves and galvanostatic charge/discharge (CD) curves of the different samples are shown in Fig. 4a and b respectively. The CV curves exhibit redox peaks in the CCFs1, CCFs2, and CCFs3, which produce Faradaic pseudo-capacitance in acidic solution. For the CCFs activated by ZnCl<sub>2</sub>, the current response first increases and then decreases with increasing ZnCl<sub>2</sub>/cotton mass ratio with the maximum occurring at ZnCl<sub>2</sub>/cotton mass ratio of 2. Comparing with the CCFs with activating by ZnCl<sub>2</sub>, the CCFs exhibit much lower current density. In the CD curves, Charge and discharge time is relatively symmetric. A transition between 0.3 and 0.5 V has been observed in CCFs2 and CCFs3, which correlates with the peaks in the CV curves due to the functional groups contributing to the electrochemical capacitance. The values of specific capacitance

calculated from the CD curves of CCFs0, CCFs1, CCFs2, and CCFs3 are 94.4, 246.7, 399.6, and 392.0  $F g^{-1}$ , respectively (determined at current density of  $1 A g^{-1}$ ). The higher specific capacitance obtained for the CCFs carbonized in  $ZnCl_2$  may mainly originate from the higher proportion of mesopores and specific surface area and may also come from the hollow structure and high concentrations of functional groups on the surface [8, 16, 17]. However, it is noted that despite the nearly same specific surface area for both CCFs2 and CCFs3, the former possess higher specific capacitance than the later, due to the higher content of the functional groups and micropore volume [16, 17]. Fig. 4c and d show the CV curves measured at different scan rates and the CD curves measured at different current densities for CCFs2. The specific capacitance values of the CCFs2 are 400.4, 387.8, 360.3, and 319.1  $F g^{-1}$  at the scan rates of 5, 10, 20, and 50  $mV s^{-1}$ , respectively. The specific capacitance values determined from the CD curves are 426.7, 399.6, 379.0, and 370.3 and 359.8  $F g^{-1}$  at the current densities of 0.6, 1, 2, 4, and 6  $A g^{-1}$ , respectively. As the scan rate and current density increase, the specific capacitance value decreases, which is related to the limited diffusion of the electrolyte ions in micropores. At high current density the micropores are not accessible to the electrolytes, hence the relative capacitance value is less than that measures at low current density.



**Fig 4.** (a) CV curves of the different samples at  $10 mV s^{-1}$ . (b) CD curves of the different samples at  $1 A g^{-1}$ . (c) CV curves of the CCFs2 at different scan rates. (d) CD curves of the CCFs2 at different current densities.

Fig. 5 shows the specific capacitance values vs. cycle number of CCFs in 1 M  $H_2SO_4$ , which were measured at the current density of  $4 A g^{-1}$ . The cyclability in Fig.5 indicates that CCFs2 have high operation stability. The capacitance retention of the CCFs1, CCFs2, and CCFs3 after 5000 cycles reaches 92.4%, 102.5%, and 94.1%, respectively. The present work shows that CCFs made by  $ZnCl_2$  activating possess excellent electrochemical performance, including high specific capacitance and high operation stability in acidic electrolyte. The excellent electrochemical performance can be mainly ascribed to the higher mesopore ratio, high specific surface area, and high concentration of the

functional groups of CCFs activated with by  $\text{ZnCl}_2$ . Compared to the preparation of activated carbon with KOH activation, the present one-step process by  $\text{ZnCl}_2$  activation is simpler and more environment-friendly.

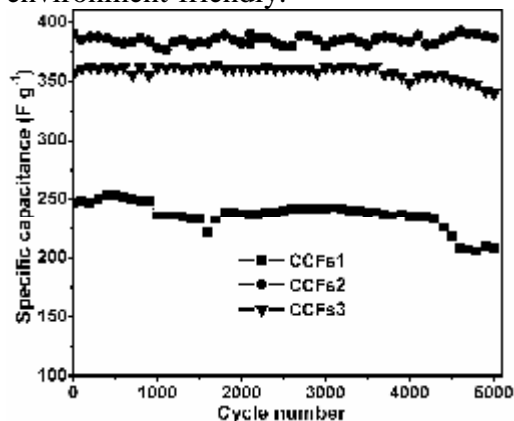


Figure 5. Operation stability of different CCFs.

## Conclusion

In conclusion, cotton-based porous carbon fibers have been prepared by a facile, cost-effective and one step carbonization and activation process.  $\text{ZnCl}_2$  used as the activation agent can improve the specific surface area and form porous structure due to the chemical activation. Due to high specific surface area, high content of oxygen functional groups, tubular structure, higher mesopore ratio, porous carbon fibers demonstrate high specific capacitance, suggesting a promising electrode material for supercapacitors.

## Acknowledgements

This work was supported by National Natural Science Foundation of China (No. 51272057), and Shenzhen Basic Research Program (JCYJ20160318093244885).

## References

- [1] E. Frackowiak, *Phys. Chem. Chem. Phys.*, 9, 1774-1785 (2007).
- [2] P. Simon and Y. Gogotsi. *Nat. Mater.*, 7, 845-854 (2009).
- [3] L. L. Zhang and X. S. Zhao. *Chem. Soc. Rev.*, 38, 2520-2531 (2009).
- [4] L. Zhao, Y. J. Qiu, J. Yu, X. Y. Deng, C. L. Dai and X. D. Bai. *Nanoscale*, 5, 4902-4909 (2012).
- [5] J. P. Liu, J. Jiang, C. W. Cheng, H. X. Li, J. X. Zhang, H. Gong and H. J. Fan. *Adv. Mater.*, 23, 20762081 (2011).
- [6] J.P. Li, Z.R. Ren, Y.Q. Ren, L. Zhao, S.G. Wang and J. Yu. *RSC Adv.*, 4, 35789-35796 (2014).
- [7] G. F. Cai, J. P. Tu, J. Zhang, Y. J. Mai, Y. Lu, C. D. Guab and X. L. Wang. *Nanoscale*, 4, 5724-5730 (2012).
- [8] S.G. Wang, Z.H. Ren, J.P. Li, Y.R., L. Zhao, J. Yu. *RSC Adv.*, 4, 31300-31307 (2014).
- [9] J. L. Xue, Y. Zhao, H. H. Cheng, C. G. Hu, Y. Hu, Y. N. Meng, H. B. Shao, Z. P. Zhang and L. T. Qu. *Phys. Chem. Chem. Phys.*, 15, 8042-8045 (2013).
- [10] C. Tran and V. Kalra. *J. Power Sources*, 235, 289-296 (2013).
- [11] A. G. Pandolfo and A. F. Hollenkamp. *J. Power Sources*, 157, 11-27 (2006)
- [12] S. Alvarez, J. Esquena, C. Solans and A. B. Fuertes. *Adv. Eng. Mater.*, 6, 897-899 (2004).
- [13] Y. J. Qiu, J. Yu, G. Fang, H. Shi, X. S. Zhou and X.D. Bai. *J. Phys. Chem. C*, 113, 61-68 (2009).
- [14] K.S. Kim, S.J. Park. *J. Power Sources*, 244, 792-798 (2013).
- [15] X.J. He, P.H. Ling, J.H. Qiu, M.X. Yu, X.Y. Zhang, C. Yu, M.D. Zheng. *J. Power Sources*, 240, 109-113 (2013).

- [16] L.Z Fan , S.Y Qiao, W.L. Song, M. Wu, X.B. He, X.H. Qu. *Electrochim. Acta*, 105, 299-304 (2013).
- [17] E. Raymundo-Pinero, K. Kierzek, J. Machnikowski and F. Beguin. *Carbon*, 44, 2498-2507(2006).